Environ. Sci. Technol. **1999**, *33,* 2081−2087

Photoassisted Degradation of Dye Pollutants. 8. Irreversible Degradation of Alizarin Red under Visible Light Radiation in Air-Equilibrated Aqueous TiO_2 Dispersions

GUANGMING LIU, TAIXING WU, AND JINCAI ZHAO*

Institute of Photographic Chemistry, Chinese Academy of Sciences, Beijing 100101, China

HISAO HIDAKA

Frontier Research Center for the Earth Environment Protection, Meisei University, 2-1-1 Hodokubo, Hino, Tokyo 191, Japan

NICK SERPONE

Department of Chemistry & Biochemistry, Concordia University, Montreal, Canada H3G 1M8

Alizarin red undergoes rapid photoassisted decomposition in air-equilibrated aqueous TiO_2 dispersions under visible light radiation ($\lambda > 420$ nm). Proton NMR, chemical oxygen demand (COD_{Cr}), UV−visible, IR, GC−MS, and spin-trapping ESR spectroscopic techniques were employed to obtain details of the photodegradation of alizarin red. Peroxides and carbonyl species are the first intermediates observed during the process. The major component of the peroxides produced is H_2O_2, and no organoperoxides were detected. We have also confirmed that in addition to CO_2 and to smaller carbonyl species the principal intermediate produced is phthalic acid, which is unable to degrade further because it does not absorb the actinic visible light radiation ($\lambda > 420$ nm). The photodegradation kinetics are discussed in terms of the Langmuir−Hinshelwood model, a case of saturation type kinetics. A mechanism for the photoassisted degradation of alizarin red mediated by TiO_2 particles under visible light radiation is proposed.

Introduction

During the past decade, much attention has been paid to investigations into the photocatalytic degradation of organic pollutants with TiO_2 particles under UV light radiation (*1*−*8*). While artificial UV light sources typically consume large quantities of electrical power, they are expensive and often unstable. Less than ca. 5% of the solar energy reaching the earth's surface is ultraviolet light. All these factors place some limitations on the application of TiO_2 in the treatment of wastewaters. Therefore, many studies have focused on the search for novel methods that can utilize visible light or sunlight for the treatment of pollutants with TiO_2 particles.

The textile and photographic industries produce dye pollutants that are becoming a major source of environmental contamination (*9*). In China, above 1.6×10^9 m^3 dye-containing wastewater/year drains into environmental water systems without treatment. These dyes absorb visible light. Earlier studies (*10*, *11a*) focused mostly on electron-transfer processes occurring between dyes and such semiconductors as TiO_2; only a few studies (*11b*−*14*) reported that dyes can photodecompose to CO_2 under visible light radiation in aqueous TiO_2 suspensions.

The mechanism of the photoassisted degradation by visible radiation is different from the pathway implicated under UV light radiation. In the former case, dyes rather than TiO_2 particles are excited by visible light to appropriate singlet and triplet states, subsequently followed by electron injection from the excited dye* onto the conduction band of TiO_2, whereas the dyes are converted to the cationic dye radicals $dye^{\bullet+}$. The injected electron TiO_2 (e^-) reacts with preadsorbed O_2 to form oxidizing species ($O_2^{\bullet-}$, $HOO^{\bullet}$, and then $^{\bullet}OH$ radicals) that can bring about photooxidations. Thus, TiO_2 plays an important role in electron-transfer mediation, even though itself is not excited.

However, the detailed irreversible photodegradation mechanism and the formation of intermediates in the degradation process have not been clarified yet. In this present study, alizarin red was chosen as the target pollutant for the photodegradative study carried out under visible light radiation in aqueous TiO_2 dispersions. The irreversible degradation process was examined by UV−visible spectroscopy, ^1H NMR spectroscopy, electron spin resonance spectroscopy (ESR), infrared (IR), and GC−MS spectroscopies together with COD assays and photoefficiency measurements. First observations indicated the formation of peroxide and carbonyl intermediates. Specifically, the formation of the $^{\bullet}OH$ radical, the determination of the peroxide components and the major intermediates, the extent of mineralization, and the related photoefficiency of the process were examined. We also treat the photodegradation kinetics using the simple Langmuir−Hinshelwood model to describe process dynamics. A photoassisted oxidation mechanism for alizarin red is proposed on the basis of the experimental results.

Experimental Section

Materials. TiO_2 photocatalyst P25 was kindly supplied by Degussa Co. The reagent 5,5-dimethyl-1-pyrroline-*N*-oxide (DMPO), used as the spin-trapping agent, was purchased from the Sigma Chemical Co. The POD reagent was made by dissolving 10 mg of horseradish peroxidase (POD; Huamei Biologic Engineering Co., China) in 10 mL of triple distilled water. The DPD reagent was composed of 0.1 g of *N*,*N*-diethyl-*p*-phenylenediamine (DPD) (Merck, p.a.) dissolved in 10 mL of 0.05 M H_2SO_4. Alizarin red and other chemicals were of analytical grade and used without further purification. Deionized and double distilled water was used throughout this study unless noted otherwise. The pH of the solutions was adjusted by diluted aqueous solutions of NaOH or $HClO_4$. For reference, the structure of alizarin red is shown below; small letters identify the protons for NMR purposes.

Photoreactor and Light Source. A 500-W halogen lamp (Institute of Electric Light Source, Beijing) was positioned inside a cylindrical Pyrex vessel; it was surrounded by a recirculating water jacket (Pyrex) to cool the lamp. A cutoff filter was placed outside the Pyrex jacket to completely remove wavelengths shorter than 420 nm and to ensure that irradiation was achieved by visible light wavelengths only.

* Corresponding author fax: +86-10-6487-9375; phone: +86-10-64888151; e-mail: jczhao@ipc.ac.cn.

10.1021/es9807643 CCC: $18.00
Published on Web 05/06/1999

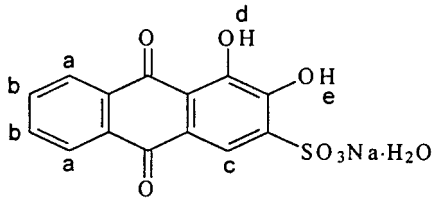

Alizarin red

The reactor used was designed to ensure a constant supply of atmospheric oxygen to the reaction volume.

Procedures and Analyses. Aqueous TiO_2 dispersions were prepared by the addition of 50 mg of TiO_2 powder to 50 mL of dye solution (2×10^{-4} M). At given irradiation time intervals, 3-mL aliquots were sampled, centrifuged, and subsequently filtered through a Millipore filter (pore size 0.22 μm) to remove TiO_2 particles. The filtrates were analyzed by UV−visible spectra with a Shimadzu-160A spectrophotometer. Chemical oxygen demand measurements were carried out by the potassium dichromate titration method (*15*) (hereafter referred to as COD_{Cr}) using two different but otherwise equivalent procedures: in the first method, COD_{Cr} values in the bulk solution were obtained after removal of TiO_2 particles; in the second method, the COD_{Cr} values were obtained by direct measurements in the TiO_2 suspensions (total COD_{cr} changes both in the bulk solution and on the TiO_2 surface). Electron paramagnetic resonance (ESR) signals of radicals spin-trapped by DMPO were examined with a Brucker ESP 300E spectrometer; the irradiation source was a Quanta-Ray Nd:YAG pulsed laser system ($\lambda = 532$ nm; 10 Hz). To minimize measurement errors, the same quartz capillary tube was used throughout for ESR measurements. Proton NMR spectra recorded during the photodegradation of alizarin red were obtained with a Varian 300 NMR spectrometer. Samples for proton NMR spectra were prepared as follows: several dispersions (50 mL; 1.0×10^{-3} M) consisting of alizarin red and100 mg of TiO_2 particulates were irradiated at different time intervals. Subsequently, TiO_2 particles were removed by the method described above. After removal of the solvent from the filtrates (below 323 K) under reduced pressures, the residues were dissolved in 0.5 mL of DMSO-d_6. Samples for gas chromatography−mass spectroscopy (GC−MS; Trio-2000, column BPX70, size 28 m × 0.25 mm) experiments were prepared in a manner otherwise identical to that for proton NMR, except that the final dried residue was dissolved in methanol. Samples prepared for infrared spectra (FTS165) were also prepared by a method similar to that for proton NMR, except that the residue was used directly. Ion chromatography (Shimadzu LC-10AS) was used to assay the quantity of SO_4^{2-} ions formed in the photodegradation of 2×10^{-4} M alizarin red solution containing 100 mg of TiO_2 particulates.

The concentration of total peroxides (including organoperoxides and H_2O_2) formed during irradiation of the 2×10^{-4} M alizarin red dispersion (50 mL; 100 mg TiO_2) was determined by a photometric method described in the literature (*16*). The quantity of carbonyl compounds in the degraded solution was determined by the 2,4-dinitrophenylhydrazine method (*17*, *18*).

Photoefficiencies (herein symbolized as ξ) of the photodegradation of alizarin red dye under visible and UV radiation were determined at 420 nm using a Japan Optical Co. interference filter that cutoff wavelengths below 410 nm and above 430 nm and determined at 365 nm using the same filter that cutoff wavelengths below 355 nm and above 375 nm, respectively. The photon flow of the 500-W halogen lamp at 420 nm was 6.8×10^{-9} einstein s^{-1} determined by Reineckate actinometry (0.008 M, 50 mL, $\xi = 0.31$; *19*), and

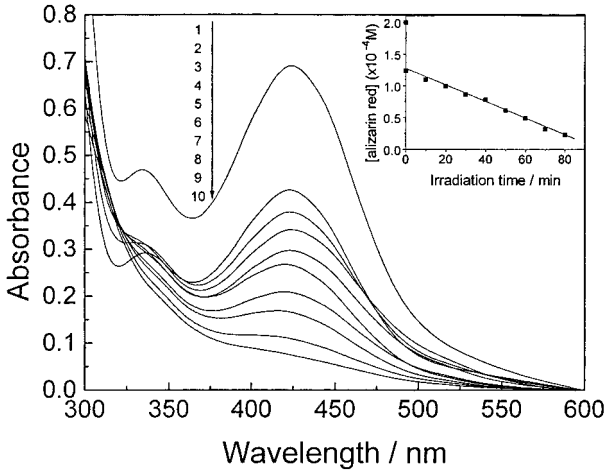

FIGURE 1. UV−visible spectral changes of alizarin red (2.0×10^{-4} M, 50 mL, pH = 3.8) in TiO_2 (50 mg) dispersions as a function of irradiation time. Spectra 2−10 denote the irradiation times 0, 10, 20, 30, 40, 50, 60, 70, and 80 min, respectively. Spectrum 1 is the UV−visible spectrum of alizarin red before the addition of TiO_2 particulates to the solution. Inset: Alizarin red concentration changes with irradiation time under the same conditions.

the photon flow of the 100-W Hg lamp at 365 nm was 5.4×10^{-9} einstein s^{-1} also assessed by Reineckate actinometry (0.0011 M, 50 mL, $\xi = 0.29$; *19*). For the degradation of alizarin red under visible or UV radiation, photoefficiencies were measured by observation of the changes in absorption spectra using a 50-mL dispersion containing 2×10^{-4} M alizarin red and 100 mg of TiO_2 under the same conditions as those employed for the photon flow measurements.

Results and Discussion

Degradation Rate and Products. The temporal absorption spectral changes taking place during the photocatalytic degradation of alizarin red mediated by TiO_2 particles under visible light radiation are displayed in Figure 1. Alizarin red shows a major absorption band at 420 nm (curve 1). Upon addition of TiO_2 particles, the absorbance decreased by ca. 38% (curve 2), reflecting the extent of adsorption of alizarin red on the TiO_2 surface in the dark. Visible light irradiation ($\lambda > 420$ nm) of the aqueous alizarin red/TiO_2 dispersion caused absorption to decrease with increase in irradiation time. The well-defined absorption bands disappeared after irradiation for ~80 min, indicating that alizarin red had degraded in the presence of TiO_2 particles. The corresponding temporal changes in the concentration of alizarin red are illustrated in Figure 1 (inset).

The photoefficiency ($\xi = 0.041$) for the degradation induced by visible radiation was ca. 5 times greater than ξ (= 0.0077) by UV irradiation. The process followed apparent zero-order kinetics: rate constant $k_d = 1.3 \times 10^{-6}$ mol L^{-1} min^{-1} ($t_{1/2} \sim 49$ min). For comparison, blank experiments carried out on an alizarin red solution containing no TiO_2 particles or on an alizarin red/TiO_2 dispersion in the dark under otherwise identical conditions showed that, in the absence of TiO_2, visible light illumination of the alizarin red solution does not degrade the dye in ≤80 min; as well, no spectral changes were seen for the alizarin red/ TiO_2 dispersion in the dark.

COD_{Cr} values reflect the amount of organic substances in the bulk solution or in the dispersion and the degree to which degradation or mineralization of the organic substrates has taken place during the irradiation period. The initial concentration of alizarin red was 4×10^{-4} M so as to minimize COD_{Cr} measurement errors. As depicted in Figure 2, COD_{Cr} values of the irradiated alizarin red/TiO_2 suspensions (curve

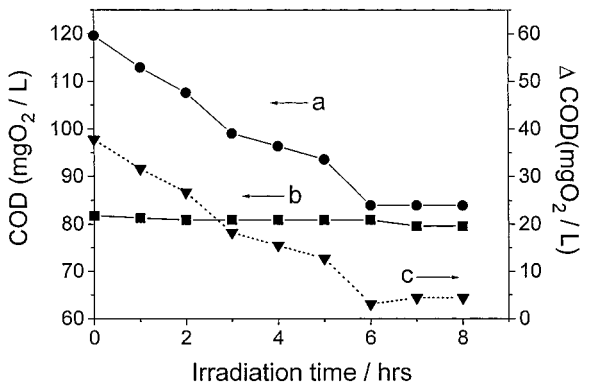

FIGURE 2. Chemical oxygen demand (as COD_{Cr}, see text) data in the photodegradation of alizarin red (4×10^{-4} M, 50 mL, pH = 3.8) versus irradiation time in the presence of TiO_2 particles (100 mg). Curve a: COD_{Cr} of the entire suspension; curve b: COD_{Cr} of the bulk solution after removal of the TiO_2 particles; curve c: representation of the difference between curves a and b. Curve c also reflects the quantity of alizarin red and intermediates adsorbed on the TiO_2 particles.

a) decreased with increasing illumination time, indicating that alizarin red was partially mineralized under visible radiation. Once the dispersion was discolored however, the COD_{Cr} of the dispersion no longer changed. These results support the visible irradiation mechanism proposed earlier (*11b*−*14*); only those organic species that can be excited by visible light can be degraded with the assistance of TiO_2 particles.

After removal of TiO_2, the COD_{Cr} of the bulk solution (curve b) showed little if any decrease with increasing illumination, indicating that COD_{Cr} values of organic species that desorbed from the TiO_2 surface to the bulk solution are nearly the same as the COD_{Cr} values of those species that adsorbed onto the TiO_2 surface from the bulk solution.The difference between the COD_{Cr} of the dispersion and of the bulk solution (e.g., ΔCOD_{Cr} values; curve c) decreased with an increase in irradiation time, reflecting the decrease in the COD_{Cr} of those organic substrates that were adsorbed on the TiO_2 surface (dye plus intermediates). That COD_{cr} of alizarin red dispersion decreased by ca. 30% (mineralization yield) after irradiation for 8 h indicates that the dye was at least partly mineralized to CO_2 in the process, consistent with CO_2 measurements obtained in earlier studies on the photodegradation of other dye pollutants under visible radiation (*12*).

The concentration of SO_4^{2-} ions formed in the degraded solution was assayed by ion chromatography. Results showed that the extent of alizarin red converted into SO_4^{2-} was ca. 35.2% after 60 min of irradiation and ca. 43% after 120 min of irradiation, respectively. Further irradiation on this discolored solution led to no increase of SO_4^{2-} ions. The lesser than expected stoichiometric SO_4^{2-} ions under the conditions used in the photoconversion arise, at least partly, from a strong adsorption of SO_4^{2-} ions on the TiO_2 surface as evidenced by a control experiment.

Formation of Intermediates. The fate of the alizarin red/TiO_2 system under degradative conditions was also examined by ESR spectroscopy to monitor the nature of the radicals that might have formed during photodegradation by visible radiation. The results show the clear signature of DMPO−$^{\bullet}$OH adducts: 1:2:2:1 quartet pattern; a = 15G (*3*, *13*, *20*). The existence of the $^{\bullet}$OH radical is closely related to the degradation of the dye by visible radiation. The ESR spectral signals of $^{\bullet}$OH radicals for the alizarin red/TiO_2 dispersion irradiated with a pulsed laser (10 Hz; excitation wavelength, 532 nm) increased in intensity in the first 5 min and remained unchanged for 2 h in the dark after irradiation was stopped.

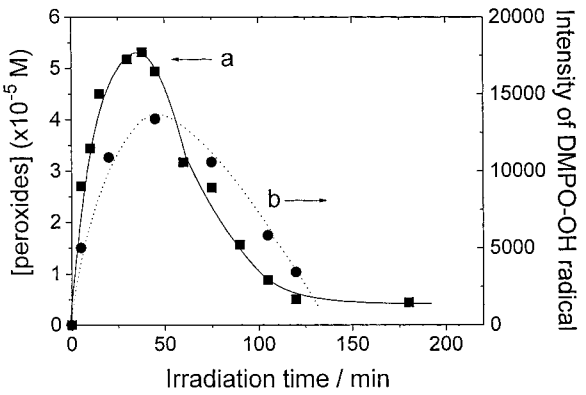

FIGURE 3. (a) Intermediate formation of peroxides in the photooxidation of alizarin red solution (2×10^{-4} M, 50 mL, pH = 3.8) with TiO_2 particulates (100 mg). (b) Changes of intensity of the signal of DMPO−$^{\bullet}$OH adduct after addition of DMPO and Fe^{3+} to the filtrates of alizarin red/TiO_2 dispersions irradiated for different time intervals by visible light (halogen lamp).

Formation and decay of peroxides produced during the photodegradation of the dye/TiO_2 dispersions (Figure 3, curve a) followed first-order kinetics: $k_r = 6.2 \pm 0.6 \times 10^{-2}$ min^{-1} ($t_{1/2}$ = 11 min) and $k_d = 2.5 \pm 0.2 \times 10^{-2}$ min^{-1} ($t_{1/2}$ = 28 min). The maximal concentration of peroxides (5.3×10^{-5} M) was reached after ca. 40 min of irradiation. Decay of the peroxide was nearly complete after ~2 h of irradiation. The total amount of peroxides measured by the DPD method may include H_2O_2 and organoperoxides (ROOH) (*16*). Hydroxyl radicals are produced when H_2O_2 reacts with iron(III) (*21*, *22*). Hence if peroxides formed in our system included H_2O_2, it could be detected by the characteristic 1:2:2:1 quartet pattern of DMPO−$^{\bullet}$OH adducts observed in the ESR spectra on addition of Fe^{3+} to the system. The concentration of Fe^{3+} was kept low to decrease the effect of the ESR signature of DMPO−Fe^{3+} (*23*). In the blank experiment, we detected no signal in a solution of DMPO and Fe^{3+} when [Fe^{3+}] was less than 2.5×10^{-5} M. Moreover, after addition of DMPO to filtrates of the degraded dispersion, samples displayed no ESR signals. However, the characteristic 1:2:2:1 quartet pattern of DMPO−$^{\bullet}$OH adducts was clearly evidenced when both DMPO and Fe^{3+} were added to the filtrates ([Fe^{3+}] = 2.5×10^{-5} M). The intensity of the DMPO−$^{\bullet}$OH signal increased with irradiation time and then decreased after reaching a maximum value after 45 min (curve b); this agrees with the formation of peroxides determined by the DPD method.

An organoperoxide can cleave and produce organic radicals by reaction with Fe^{3+} as noted in reactions 1−3 (*23*):

$$\mathrm{ROOH} + \mathrm{Fe^{3+}} \rightarrow \mathrm{Fe^{2+}} + \mathrm{ROO^{\bullet}} + \mathrm{H^{+}} \quad (1)$$

$$\mathrm{Fe^{2+}} + \mathrm{ROOH} \rightarrow \mathrm{Fe^{3+}} + \mathrm{RO^{\bullet}} + \mathrm{OH^{-}} \quad (2)$$

$$\mathrm{RH} + \mathrm{RO^{\bullet}} \rightarrow \mathrm{ROH} + \mathrm{R^{\bullet}} \quad (3)$$

These organic radicals (ROO$^{\bullet}$, RO$^{\bullet}$, R$^{\bullet}$) can be trapped by DMPO and produce the corresponding ESR signals of DMPO−$^{\bullet}$OR or DMPO−$^{\bullet}$R and/or DMPO−$^{\bullet}$OOR adducts (*24*, *25*). We detected no characteristic ESR signals for any of these radical adducts in the system under otherwise identical conditions as above. Evidently, the concentration of the organoperoxides must be below the detection limits of our instrument. or else the organoperoxides formed must be chemically unstable, easily decomposing in aqueous solution. We deduce that the main component of the peroxides formed in the degraded solution is H_2O_2.

Proton NMR spectra of the degraded solution after irradiation at various time intervals are reported in Figure 4.

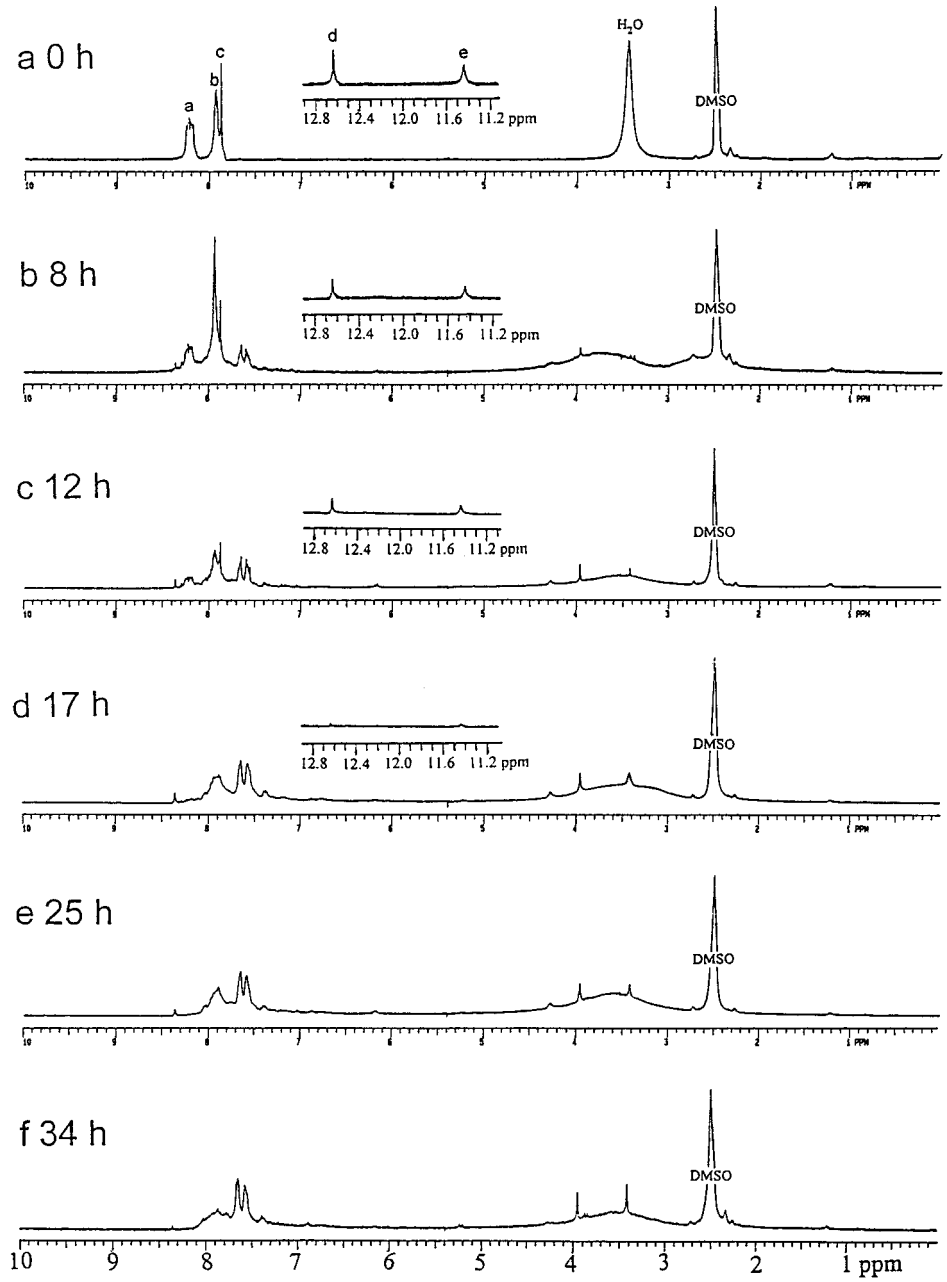

FIGURE 4. Temporal ^{1}H NMR spectral profiles of the changes occurring during the photodegradation of alizarin red solution (1×10^{-3} M, 50 mL, pH = 3.8) in the presence of TiO_2 (100 mg) at various irradiation times.

Spectrum a illustrates the proton NMR signals of pure alizarin red before irradiation and the related assignments of the various proton chemical shifts (see above for the structure of alizarin red) in keeping with standard spectra found in the Sadtler NMR Atlas.

During the time evolution of the degradation process (spectra b−f of Figure 4), a sequence of new signals at δ 7.5−7.8, 3.97, and 3.43 ppm appeared and increased with increasing irradiation time. While the characteristic signals of alizarin red at δ 7.8−8.4 ppm (aromatic protons; a−c) and at δ 11.2−12.8 ppm (OH protons; d and e) disappeared, some new aromatic compounds (δ 7.5−7.8 ppm) formed during the degradation process. We attribute the species displaying the latter signals at δ 7.5−7.8 ppm to phthalic acid (see also GC−MS results below). It should be noted that, after 17 h of irradiation, the peaks of the two phenolic OH groups at δ 11.2−12.8 ppm completely disappeared whereas the aromatic peaks at δ 7.8−8.4 ppm were still visible after this time, indicating that the hydroxyl groups of alizarin red are more easily attacked by active oxygen species than the benzene ring of the dye during the initial irradiation stages.

The temporal variation of the carbonyl groups of alizarin red during its photodegradation mediated by TiO_2 particles is shown in Figure 5. The two carbonyl groups of alizarin red react with 2,4-dinitrophenylhydrazine in alkaline media to form the corresponding 2,4-dinitrophenylhydrazone derivative that displays two major absorption bands at 550 and 600 nm (spectrum 1 of Figure 5A), different from the analogous spectra of small carbonyl compounds (absorption bands at 430 and 520 nm; *17*, *18*). Such a large red shift of the absorption in the phenylhydrazone derivative is due to the larger conjugated benzene ring in alizarin red.

Visible light irradiation of the aqueous alizarin red/TiO_2 dispersion caused the carbonyl concentration of alizarin red to decrease via zero-order kinetics $k_d' \sim 2.9 \times 10^{-5}$ mol L^{-1} h^{-1} (Figure 5B, curve b), concomitantly with the growth of new bands at ca. 430 nm (note the clean isobestic point at 490 nm, Figure 5A). The new absorption band is the same

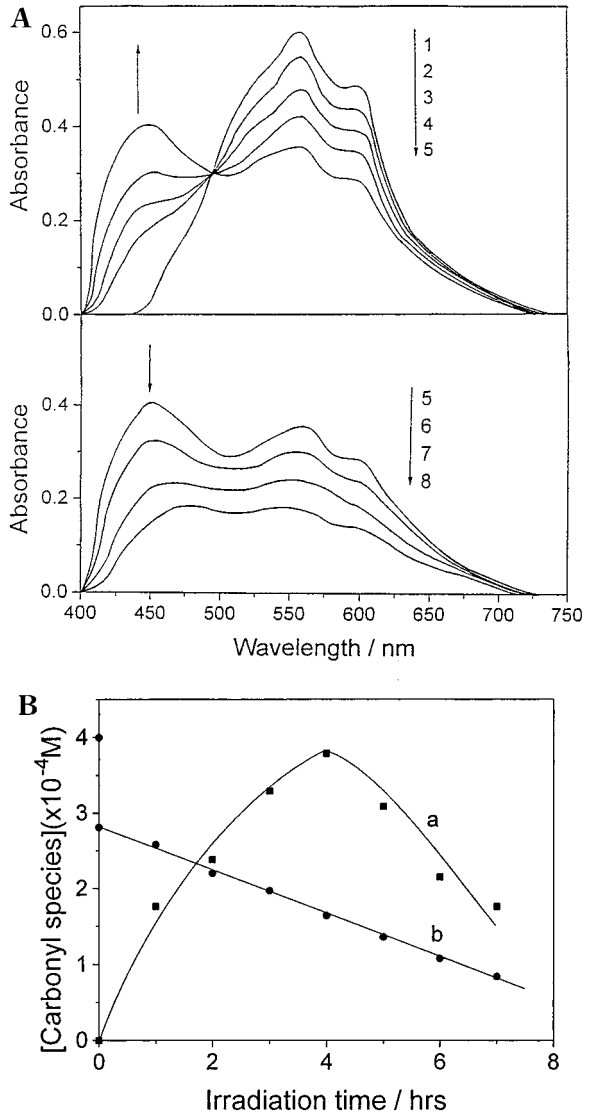

FIGURE 5. (Panel A) Variation in absorption spectra of complexes of 2,4-dinitrophenylhydrazine and carbonyl compounds formed in the photodegradation of alizarin red (4×10^{-4} M, 50 mL, pH = 3.8) in the presence of TiO_2 particles (100 mg) under visible light irradiation. Spectra 1−8 denote the irradiation times 0, 1, 2, 3, 4, 5, 6 and 7 h, respectively. (Panel B) (a) Concentration changes of the new carbonyl intermediate(s) as a function of irradiation time under the same conditions. (b) Concentration changes of the dye carbonyl compound as a function of irradiation time under the same conditions.

as the one described by Lappin et al. (*17*) and by Jordan and co-workers (*18*), representing the characteristic absorption peaks of the 2,4-dinitrophenylhydrazone derivative with small carbonyl compounds. To the extent that carboxylic acids (e.g., phthalic acid) do not react with 2,4-dinitrophenylhydrazine, the new absorption band must then be due to some new carbonyl compounds (e.g., aldehydes and/or ketones) formed during the degradation process and degrade via first-order kinetics: $k_r \sim 0.37$ h^{-1} and $k_d \sim 0.26$ h^{-1}, respectively. After 4 h of irradiation, the new band at 430 nm and the one resulting from alizarin red at 550 nm decreased with irradiation time (Figure 5A), indicating ultimate degradation of intermediates on further irradiation (Figure 5B, curve a).

The temporal course of the photoassisted degradation of alizarin red was also monitored by IR spectroscopic methods (Figure 6). Bands of characteristic carbonyl absorptions of the anthraquinone dye (1670−1630 cm^{-1}) and the benzene ring (1400−1600 cm^{-1}) decreased with irradiation time; after

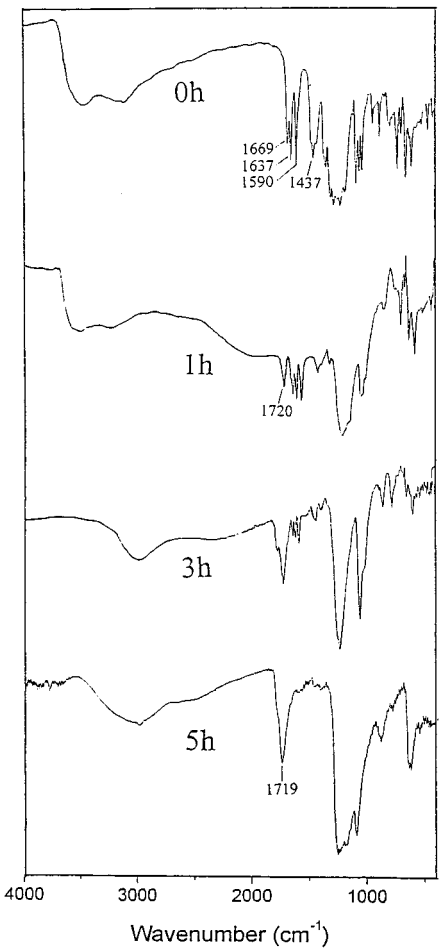

FIGURE 6. Variation of IR spectra in the photodegradation of alizarin red (4×10^{-4} M, pH = 3.8) in the presence of TiO_2 particles (100 mg) under visible light irradiation.

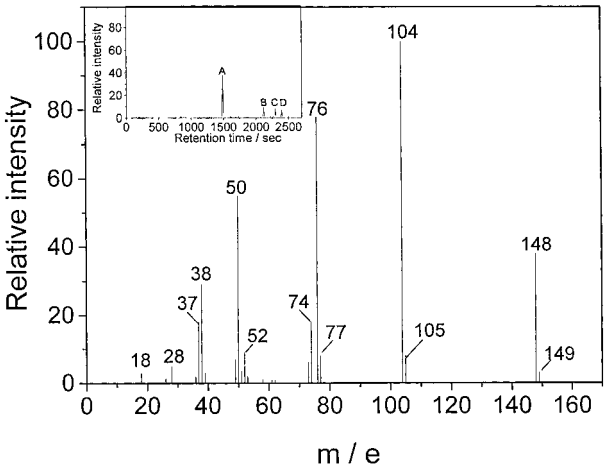

FIGURE 7. Mass spectra of the main component of completely degraded products (from GC−MS spectroscopy). Inset: Gas chromatogram of a completely degraded alizarin red aqueous solution.

∼ 5 h the absorptions of the C═O groups pertaining to the dye disappeared while the −C═C− absorptions of the phenyl ring decreased only partially (see GC−MS results in Figure 7). A strong new IR peak attributable to C═O groups of carboxylic acids, aldehydes, and/or ketones appeared at 1720 cm^{-1} whose intensity increased with increasing irradiation time. According to GC−MS results, the absorption band at 1720 cm^{-1} is likely due to the C═O groups of phthalic acid;

SCHEME 1. Proposed Photodegradation Mechanism for Alizarin Red under Visible Light Radiation

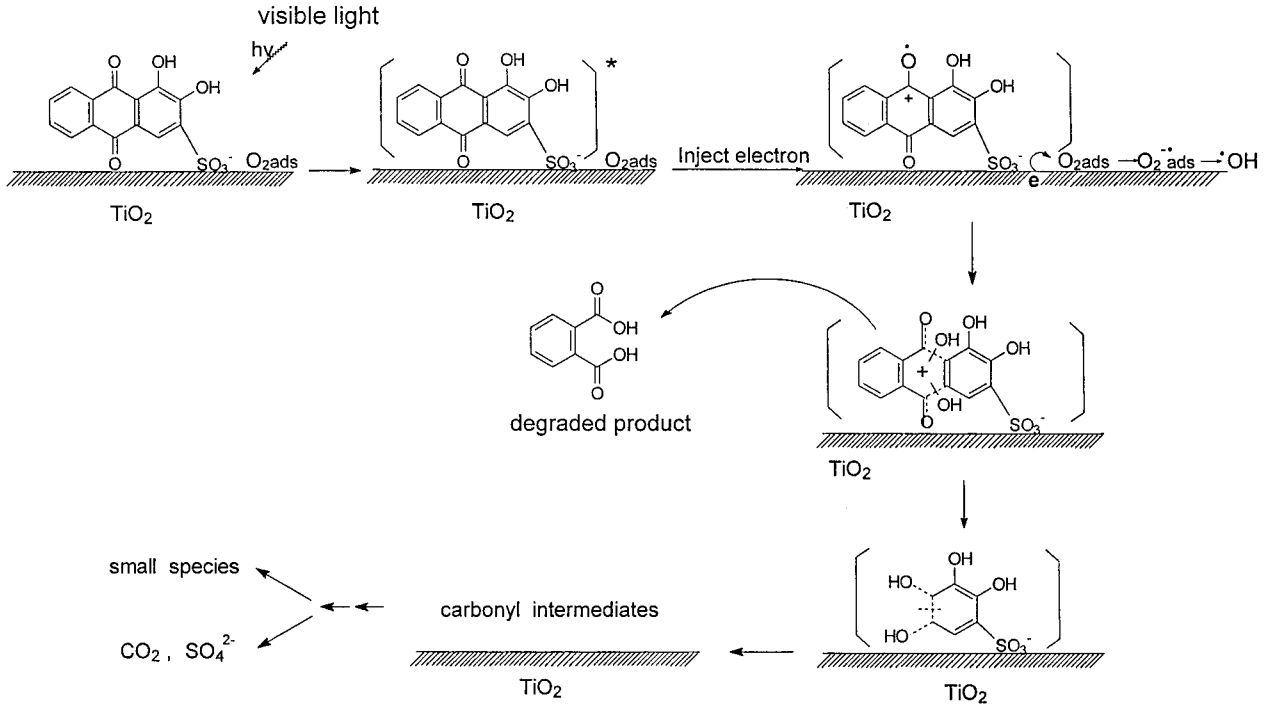

no variation of C═O groups of aldehyde and/or ketone intermediates (Figure 5) could be observed because of strong and broad absorptions by the C═O of phthalic acid.

To further confirm the intermediate species suggested above, we examined the final degraded products of alizarin red by GC−MS techniques. The results are shown in Figure 7. The gas chromatogram (inset) shows the concomitant appearance of four components. The predominant peak (A) in the chromatogram was subjected to mass spectral analysis. The MS features confirm the major component of the degraded fragments to be phthalic acid. The complexity of the GC−MS spectra precluded further confirmation of the other components formed in the photodegradation of alizarin red.

Photodegradation Kinetics and Mechanism. The photodegradation kinetics of many organic compounds in TiO_2 dispersions under UV radiation have often been modeled using the simple Langmuir−Hinshelwood equation (*3*), which expresses the initial rate r as a function of initial concentration c (eq 4):

$$\frac{1}{r} = \frac{1}{kK}\,\frac{1}{c} + \frac{1}{k} \qquad (4)$$

where k is the apparent rate constant for the process, and K is the adsorption coefficient under irradiation conditions. Photodegradation kinetics under visible light radiation were assessed by examining the degradation rate of alizarin red at different initial concentrations. The good linear relationship between r^{-1} and c^{-1} indicates that the degradation kinetics of alizarin red also follow the L−H model, a manifestation of the more general case of saturation-type kinetics. The adsorption constant K determined from eq 4 for the process is 1.2×10^4 L mol $^{-1}$. While we obtained the adsorption coefficient $K' = 1.4 \times 10^5$ L mol^{-1} from the Langmuir equation (*26*) in the dark, the difference between K and K' was caused by the photodesorption and/or photoadsorption and by the photoreaction of the substrate on the TiO_2 surface, as reported in earlier work (*12b*).

It should be noted that the mechanism of photodegradation of dyes by visible light is significantly distinct from the pathway prevailing under UV radiation. TiO_2 particles are not excited by visible light, rather the dyes are excited. Details of the degradation of alizarin red are illustrated in Scheme 1. After photoexcitation at >420 nm, the excited dye (dye*) injects an electron to the conduction band of TiO_2 particles {$E(D^*/D^+) = -1.57$ V (*27*), $E_{cb}(TiO_2) = -0.5$ V (vs NHE); *12b*}, where it is scavenged by preadsorbed molecular oxygen to yield the superoxide radical anion, $O_2^{\bullet-}$, which on protonation produces HOO$^\bullet$ radicals in acidic media (pH = 3.8). The hydroperoxy radicals may also be one of the predominant oxidants in the initial photodegradation stages; it accepts another electron and proton to yield H_2O_2. As detected, a large quantity of H_2O_2 formed in the degraded solution (see Figure 3), although it has no effect on the degradation of the dye in the absence of TiO_2 as evidenced by a control experiment, H_2O_2 can be reduced to produce the highly reactive $^\bullet$OH radicals. Attack of HOO$^\bullet$ and $^\bullet$OH radicals on the dye molecules produces organoperoxides and/or hydroxylated intermediates. The hydroxylated aromatic ring is ultimately cleaved to form phthalic acid and other carbonyl species (e.g., aldehydes and/or ketones), suggesting that the C—C bond near the C═O group of alizarin red is readily attacked. The other multihydroxylated species (Scheme 1) decomposes further to smaller mineralized products, e.g., CO_2 and SO_4^{2-} ions, and to other smaller carbonyl species.

Acknowledgments

The authors appreciate the generous financial support of this work from the National Natural Science Foundation of China (29677019, 29637010, and 29725715), from the Foundation of the Chinese Academy of Sciences and the China National Committee for Science and Technology (to J.Z.), by a Grant-in-Aid for Scientific Research from the Japanese Ministry of Education (10640569 to H.H), and by a grant from the Natural Sciences and Engineering Research Council of Canada (A5443 to N.S.). We are also grateful to Prof. J. Chen for her measurements of the ESR spectra.

Literature Cited

(1) Fox, M. A.; Dulay, M. T. *Chem. Rev.* **1993**, *93*, 341.

(2) Ollis, D. F.; Pelizzetti, E.; Serpone, N. *Environ. Sci. Technol.* **1991**, *25*, 1523.
(3) Hidaka, H.; Zhao, J.; Pellizzetti, E.; Serpone, N. *J. Phys. Chem.* **1992**, *96*, 2226.
(4) Hidaka, H.; Asai, Y.; Zhao, J.; Pelizzetti, E.; Serpone, N. *J. Phys. Chem.* **1995**, *99*, 8244.
(5) Zhao, J.; Hidaka, H.; Takamura, A.; Pelizzetti, E.; Serpone, N. *Langmuir* **1993**, *9*, 1649.
(6) Kormann, C.; Bahnemann, D. W.; Hoffmann, M. R. *J. Phys. Chem.* **1988**, *92*, 5196.
(7) Kamat. P. V. *Chem. Rev.* **1993**, *93*, 267.
(8) Hoffmann, M. R.; Martin, S. T.; Choi, W.; Bahnemann, D. W. *Chem. Rev.* **1995**, *95*, 69.
(9) Tincher, W. C. *Text. Chem. Color.* **1989**, *21*, 33.
(10) Rossetti, R.; Brus, L. E. *J. Am. Chem. Soc.* **1984**, *106*, 4336.
(11) (a) He, J.; Zhao, J.; Shen, T.; Hidaka, H.; Serpone, N. *J. Phys. Chem.* **1997**, *101*, 9027. (b) Qu, P.; Zhao, J.; Zang, L.; Shen, T.; Hidaka, H. *Colloids Surf.* **1998**, *138*, 39.
(12) (a) Zhang, F.; Zhao, J.; Zang, L.; Shen, T.; Hidaka, H.; Pelizzetti, E.; Serpone, N. *J. Mol. Catal. A: Chem.* **1997**, *120*, 173. (b) Zhang, F.; Zhao, J.; Shen, T.; Hidaka, H.; Pelizzetti, E.; Serpone, N. *Appl. Catal. B: Environ.* **1998,** *15*, 147.
(13) (a) Zhao, J.; Wu, K.; Wu, T.; Hidaka, H.; Serpone, N. *J. Chem. Soc., Faraday Trans.* **1998**, *94*, 673. (b) Zhao, J.; Wu, T.; Wu, K.; Hidaka, H.; Serpone, N. *Environ. Sci. Technol.* **1998**, *32*, 2394.
(14) (a) Qu, P.; Zhao, J.; Shen, T.; Hidaka, H. *J. Mol. Catal. A: Chem.* **1998**, *129*, 257. (b) Wu, T.; Liu, G.; Zhao, J.; Hidaka, H.; Serpone, N. *J. Phys. Chem.* **1998**, *102*, 5845.
(15) *Chinese National Standard: GB 11914-89*, 1989.
(16) Bader, H.; Sturzenegger, V.; Hoigne, J. *Water Res.* **1988**, *22*, 1109.
(17) Lappin, G. R.; Clark, L. C. *Anal. Chem.* **1951**, *23*, 541.
(18) Jordan, D. E.; Veatch, F. C. *Anal. Chem.* **1964**, *36*, 120.
(19) Wegner, E. E.; Adamson, A. W. *J. Am. Chem. Soc.* **1966**, *88*, 394.
(20) Kochany, J.; Bolton, J. R. *J. Phys. Chem.* **1991**, *95*, 5116.
(21) Walling, C. H. *Acc. Chem. Res.* **1975**, *8*, 125.
(22) Barb, W. G.; Baxendale, J. H.; George, P.; Hargrave, K. R. *Trans. Faraday Soc.* **1951**, *47*, 591.
(23) Saprin, A. N.; Piette, L. H. *Arch. Biochem. Biophys.* **1977**, *180*, 480.
(24) Makino, K.; Hagiwara, T.; Hagi, A.; Nishi, M.; Murakami, A. *Biochem. Biophys. Res. Commun.* **1990**, *172*, 1073.
(25) Liu, Y.; Stolze, K.; Dadak, H.; Nohi, H. *Photochem. Photobiol.* **1997**, *66*, 443.
(26) Hiemenz. P. C. In *Principles of Colloid and Surface Chemistry*, 2nd ed.; Marcel Dekker: New York, 1986; p 402.
(27) Meites, L.; Zuman, P. *CRC Handbook Series in Organic Eletrochemistry*, Vol. I; CRC Press: Boca Raton, FL, 1976.

Received for review July 27, 1998. Revised manuscript received November 9, 1998. Accepted March 23, 1999.

ES9807643